

Simulation of the Dynamic Behavior of the Load Frequency Control System in the Power Network by Integrating Different Power Plants

Mohammadreza Moradian Ghazanfar Shahgholian*

Department of Electrical Engineering, Najafabad Branch, Islamic Azad University, Najafabad, Iran Smart Microgrid Research Centre, Najafabad Branch, Islamic Azad University, Najafabad, Iran

* Corresponding author, Email: shahgholiangh@gmail.com

Article Information

Article Type

RESEARCH ARTICLE

Article History

RECEIVED: 14 Jul 2025 REVISED: 29 Sep 2025 ACCEPTED: 30 Oct 2025

Published Online: 01 Nov 2025

Keywords

Interconnected power system Steam power plant Gas power plant Hydro power plant Load frequency control

Abstract

Maintaining a relatively constant frequency is crucial in power systems. The secondary control loop plays a key role in ensuring that the frequency stays close to nominal values, while also managing the power exchange between interconnected control areas through established transmission lines. This study focuses on examining and simulating the dynamic behavior of interconnected power systems. Various power system configurations are explored, incorporating steam, hydro, and gas power plants. We present MATLAB-based simulations for both two-area and three-area power systems. The results of these time-domain simulations are analyzed by calculating the eigenvalues of the power system matrix across different scenarios. The findings indicate that in response to step changes in demand load, independent areas exhibit varying frequency droop characteristics, with gas power plants showing the least frequency droop and hydro power plants displaying the most significant frequency droop.

Cite this article: Moradian, M., Shahgholian, G. (2025). Simulation of the Dynamic Behavior of the Load Frequency Control System in the Power Network by Integrating Different Power Plants. DOI: 10.22104/hfe.2024.7214.1330



© The Author(s). Publisher: Iranian Research Organization for Science and Technology (IROST) DOI: 10.22104/hfe.2024.7214.1330

1 Introduction

Energy is crucial for the advancement of industrial and commercial sectors, societal welfare, quality of life, and overall security. Studies show a strong correlation between national development and energy consumption. highlighting the importance of accessible energy resources in supporting economic growth, particularly in developing nations [1,2]. Electrical energy, in particular, is a cornerstone of industrial, economic, and social progress, with enhanced production and distribution capacities directly contributing to national development [3,4]. Electricity generation involves various types of power plants and technologies, classified by their primary energy sources. Conventional, non-renewable sources include thermal power plants such as steam, gas, combined cycle, nuclear, and diesel plants, while renewable sources include hydropower, wind, geothermal, tidal, and solar plants. In general, power plants rely on turbines and generators to produce mechanical energy, which is then converted into electricity. However, photovoltaic plants use solar cells for direct energy conversion [5, 6].

The expansion and diversification of energy sources have increased the structural complexity of modern power systems, leading to nonlinear behaviors and operational challenges, including frequency deviations, which are a critical issue [7,8]. Ensuring that frequency and voltage remain within standard values is essential for maintaining power quality [9, 10]. Power systems face continuous challenges, such as unpredictable external disturbances and uncertainties in parameters and system models, requiring robust control loops to stabilize and optimize system performance [11, 12]. Load frequency control (LFC) loops are employed to stabilize frequency at nominal levels by adjusting the generated power to match fluctuating demand, thus maintaining equilibrium in power exchanges between interconnected areas [13, 14].

To improve reliability and economic operation, modern power systems have become interconnected networks, consisting of multiple areas. In this context, when there is a difference between the generated power and the consumed load, the LFC system is responsible for balancing the generated power and the demanded load to maintain the nominal frequency of the system. It must also control the power exchange between areas based on the planned inter-area power values [15, 16].

In interconnected systems, LFC loops are essential for managing transient frequency deviations and minimizing steady-state errors, thereby enhancing system stability [17,18]. These systems offer significant advantages, such as balancing supply-demand mismatches,

integrating renewable energy sources, and accessing distant energy resources. However, they also introduce the potential for fault propagation across the network, highlighting the need for effective management and control to prevent widespread instability [19, 20]. Significant research has been devoted to enhancing the stability of LFC systems in interconnected networks [21, 22]. Topics discussed in research include adaptive load frequency control (LFC) [23], small-signal stability [24], combining algorithms and proposing a cascade proportional-integral-derivative (PID) controller [25], sliding mode control for LFC in multi-zone power systems [26], an LFC strategy based on a two-deep Qnetwork [27], and controlling voltage and frequency parameters in a multi-source power system [28]. Among advanced storage solutions, superconducting magnetic energy storage (SMES) systems provide efficient energy storage with rapid power regulation, making them highly valuable for enhancing LFC in power systems. An adaptive neural control model, based on varying control error and stored energy, has been proposed in [29] to optimize LFC, complemented by a controller that adjusts its gain using the integral square error criterion.

Additionally, model predictive control methods have been explored for multi-area interconnected systems, incorporating both photovoltaic and thermal generation. In [30], these methods optimize control signals by minimizing the weighted sum of predicted errors and future control values, thereby enhancing system dynamics.

Increased photovoltaic integration and grid connections, however, introduce disturbances caused by inverter parameters, leading to intensified frequency fluctuations. Recent strategies, such as dual equivalent-input-disturbance controllers, have shown promise in mitigating these fluctuations in multi-area power systems [31].

An isolated microgrid LFC system with uncertain renewable energy sources is investigated in [32]. A multi-objective formula is proposed to tune the controller in a microgrid with multiple energy sources, including fuel cells and battery storage. Simulation results highlight the effectiveness of the multi-objective approach in improving the system's performance and stability indices.

Wind power, as an environmentally friendly energy source, poses unique challenges to system stability due to its low inertia. A PI-structured optimal automatic generation control, based on full-state vector feedback control theory, has been applied to manage load disturbances in multi-source systems. Simulations presented in [33] demonstrate that wind power improves the load disturbance response under variable wind conditions.

Renewable energy integration reduces reliance on non-renewable resources but can disrupt frequency stability, thereby affecting power quality. Advanced controllers, such as linear active disturbance rejection control combined with a soft actor-critic algorithm, have demonstrated effectiveness in mitigating adverse effects on frequency response in two-area interconnected systems, as presented in [34].

The rising penetration of renewables has high-lighted low inertia as a critical concern in power networks. In [35], a novel three-degree-of-freedom LFC strategy for renewable-integrated interconnected systems is proposed, utilizing fractional-order control with a compensatory filter to address frequency and power deviation issues across connection lines. This study presents a dynamic analysis and simulation of LFC behavior within interconnected multi-zone systems across various power plant configurations, including steam, gas, and hydro. System matrix eigenvalue analysis is utilized to evaluate the dynamic response and system modes under different configurations. This study aims to:: compare dynamic responses across different

power plant types, analyze mode behaviors in interconnected systems with varied architectures, and examine primary frequency control responses in multi-zone systems with differing structures.

2 Load Frequency Control

Hierarchical control, as shown in Figure 1, is a common solution for damping frequency oscillations and is typically classified into three control levels: primary, secondary, and tertiary. Depending on the system conditions, the severity of the disturbance, and the degree of frequency deviation, an emergency control loop may be necessary to restore the power system frequency [36,37]. Minor frequency oscillations during normal operation of the power system are mitigated by primary control. The secondary control loop is activated based on the amount of stored power to restore frequency during abnormal operation. In the case of a severe disturbance that causes a significant imbalance between production and load demand, the tertiary control loop is employed to reduce the frequency deviation [38,39].

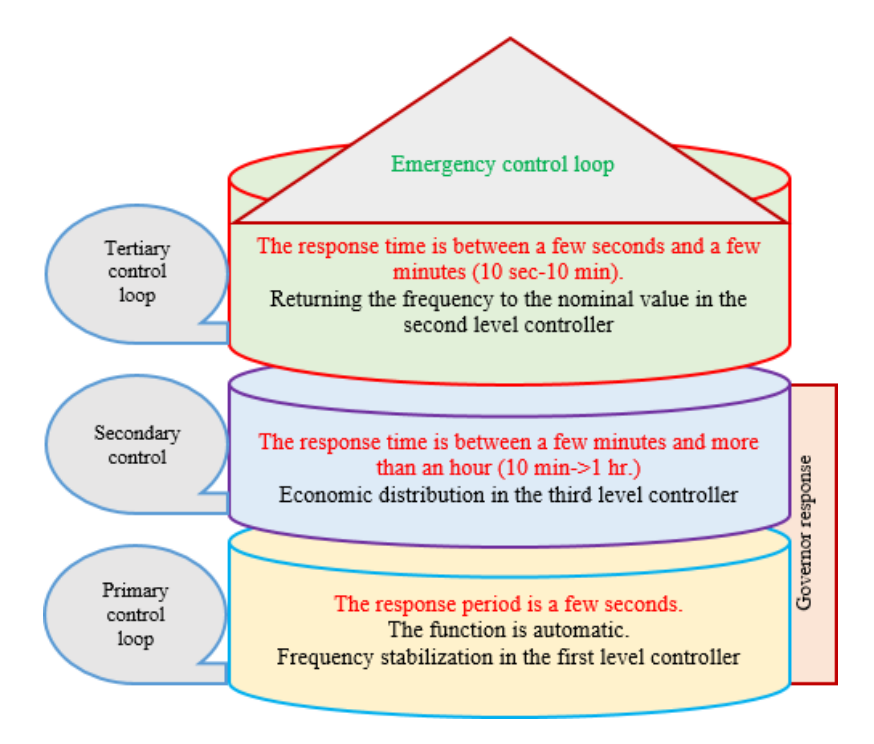


Fig. 1. Frequency control loops in the power system.

Frequency control is divided into four levels: primary level control (based on the droop properties of the system), secondary level control (involving measurement of frequency variation and power transfer be-

tween zones), tertiary control (used to reduce frequency when required by the system operator through various protection methods), and emergency control (providing continuous system control to prevent blackouts, severe outages, or cascading failures during large disturbances). A single-area power system with control loops, including an inertia control loop, is shown in Figure 2.

The virtual inertia control method is employed to assist in managing the overall inertia of the power system and enhance frequency performance [40,41].

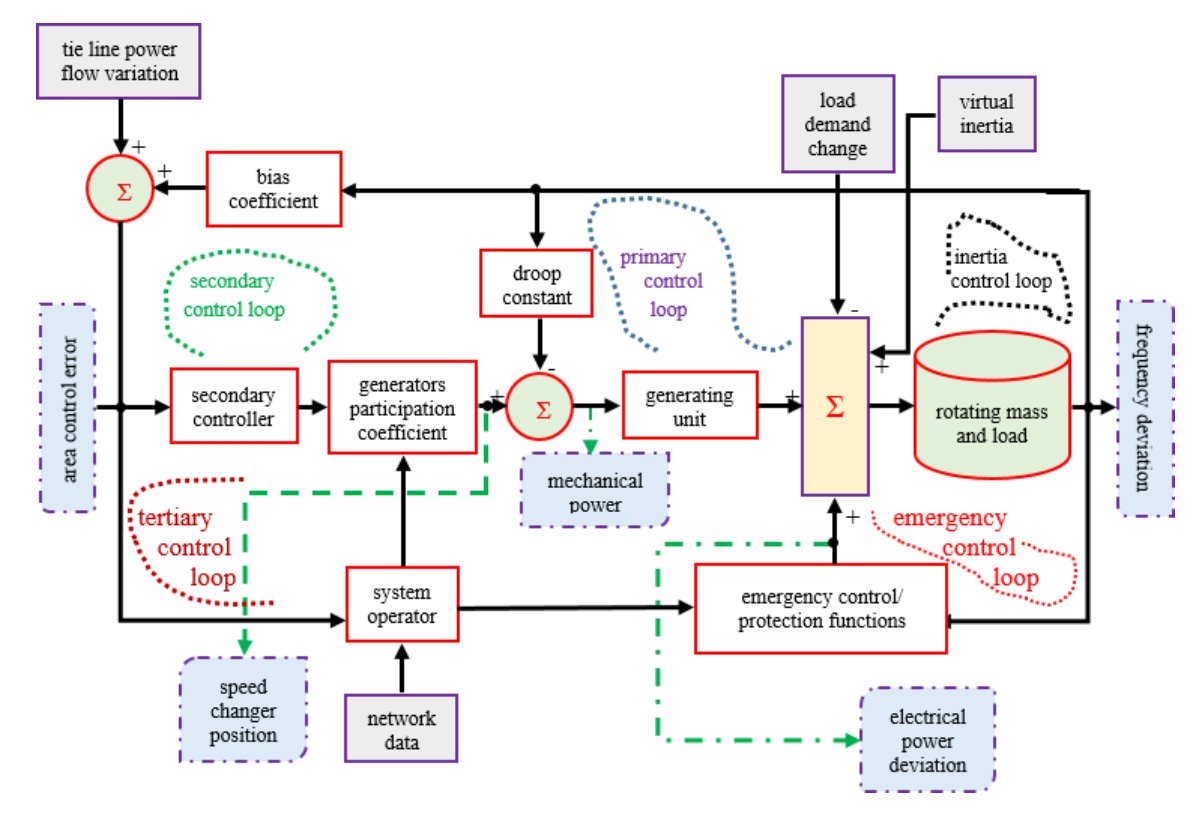


Fig. 2. Depiction of control loops in a single-zone power system.

3 Interconnected Power System Model

Low energy density, combined with the stochastic nature of energy sources and fluctuations in energy generation, has created challenges for the load frequency control system [42, 43]. The load demanded by consumers varies throughout the day, necessitating adjustments in the active power output to match load consumption, which requires precise generator output control [44, 45]. Due to the constantly changing load demand, power systems must regulate input power to maintain stability. In a multi-zone power system, it is essential to maintain the input-output balance to prevent deviations in system frequency and imbalances in transmission line power between areas [46, 47].

Figure 3 shows the connection between one area and other areas in an interconnected power system, where T_{ij} is the synchronizing torque coefficient of the tie-line between areas i and j. ΔP_d is incremental changes in load demand, Δf is incremental changes in system fre-

quency and ΔP_m is incremental changes in mechanical power. The error signal for the incremental changes in the connection line power is based on the frequency difference between the areas [48, 49]. The parameters of the studied power system are given in the Tables 1 to 3. The linearized equations representing the dynamic model of each power plant are described below. Each area has two input signals including u_1 =load demand changes (ΔP_d) and u_2 =load reference set-point. $\Delta P_{\rm tie}$ is the tie-line power flows throughout the tie-line between existing areas. The order of the system matrix (the number of state variables) to describe the power plant model in the state space is given in Table 4.

Table 1. Hydro power plant parameters.

Parameter	J_M	K_D	T_W	T_R	T_P	R_H	T_G
Value	6	1	1	5	9.5	0.2	0.2

Table 2. Steam power plant parameters.

Parameter	J_M	K_D	T_H	F_H	T_T	R_S	T_G
Value	10	1	7	0.3	0.3	0.2	0.2

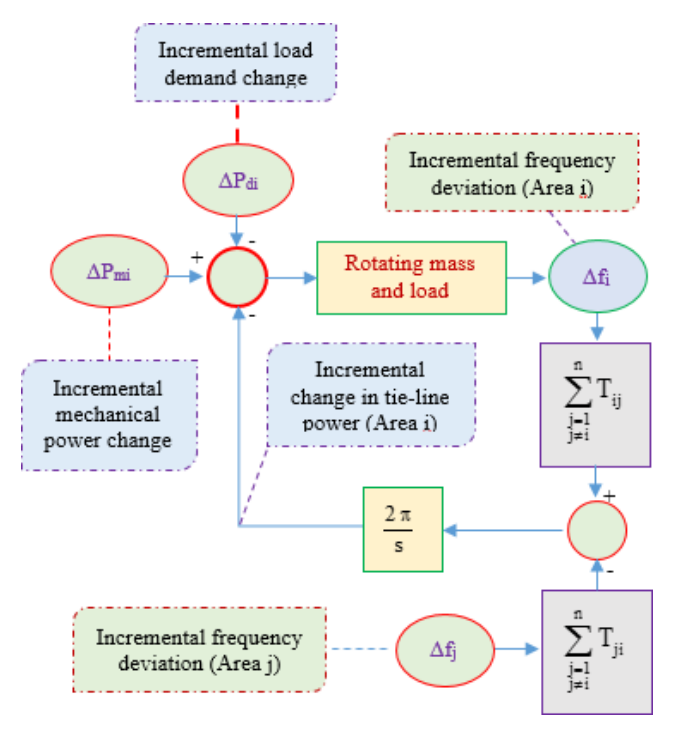


Fig. 3. Connection between adjacent areas in the interconnected power system.

Table 3. Gas power plant parameters.

Parameter	Value
J_M	8
K_D	1
T_G	1.1
T_L	0.6
R_G	0.2
T_F	0.239
$T_{\rm CR}$	0.01
$T_{ m CD}$	0.2
K_V	1
T_V	0.049

Table 4. Matrix order of state space representation system for power plants.

Power Plant	System matrix order
Steam power plant with reheater	4
Hydro power plant	4
Gas power plant	5
Steam power plant without reheater	3

3.1 Small signal model equations of hydropower in state space

To express the first-order differential equations representing the dynamic model of the hydropower plant,

four state variables are used, including x_1 = frequency changes (Δf) , x_2 = turbine output mechanical power changes (ΔP_m) , x_3 = transient droop compensation output, and x_4 =water valve changes [50].

$$\begin{split} \frac{dx_1}{dt} &= -\frac{K_D}{J_M} x_1 + \frac{K_1}{J_M} x_2 \pm \frac{1}{J_M} \sum \Delta P_{\text{tie}} \\ &- \frac{1}{J_M} u_1 \,, \\ \frac{dx_2}{dt} &= \frac{2T_R K_G}{R_H T_P T_G} x_1 - \frac{2}{T_W} x_2 + \left(\frac{2}{T_W} + \frac{2}{T_P}\right) x_3 \\ &- \left(\frac{2}{T_P} - \frac{2T_R}{T_P T_G}\right) x_4 - \frac{2K_G T_R}{T_P T_G} u_2 \,, \end{split} \tag{2} \\ \frac{dx_3}{dt} &= -\frac{K_G T_R}{R_H T_G T_P} x_1 - \frac{1}{T_P} x_3 \\ &+ \left(\frac{1}{T_P} - \frac{T_R}{T_P T_G}\right) x_4 + \frac{K_G T_R}{T_G T_P} u_2 \,, \end{split} \tag{3} \\ \frac{dx_4}{dt} &= -\frac{K_G}{R_H T_G} x_1 - \frac{1}{T_G} x_4 + \frac{K_G}{T_G} u_2 \,. \end{split} \tag{4}$$

3.2 Small signal model equations of gas power plant in state space

To display the first order differential equations in order to display the small signal model of the gas power plant, five state variables are used, which are: x_1 =frequency changes (Δf) , x_2 =compressor output power changes, x_3 =fuel system output power changes, x_4 =speed governor output power changes and x_5 =valve position output power changes.

$$\frac{dx_1}{dt} = -\frac{K_D}{J_M} x_1 + \frac{1}{J_M} x_2 \pm \frac{1}{J_M} \sum \Delta P_{\text{tie}}
- \frac{1}{J_M} u_1, \qquad (5)$$

$$\frac{dx_2}{dt} = -\frac{1}{T_D} x_2 + \frac{1}{T_D} x_3, \qquad (6)$$

$$\frac{dx_3}{dt} = \frac{T_{\text{CR}} K_V T_L}{T_V T_F R_G T_G} x_1 - \frac{1}{T_F} x_3
+ \frac{1}{T_F} \left(\frac{T_{\text{CR}}}{T_G} + 1\right) x_4 + \frac{T_{\text{CR}}}{T_G T_F} \left(\frac{T_L}{T_V} - 1\right) x_5
- \frac{T_{\text{CR}} K_V T_L}{T_F T_V T_G} u_2, \qquad (7)$$

$$\frac{dx_4}{dt} = -\frac{K_V T_L}{T_V R_G T_G} x_1 - \frac{1}{T_G} x_4
- \frac{1}{T_G} \left(\frac{T_L}{T_V} - 1\right) x_5 + \frac{K_V T_L}{T_V T_G} u_2, \qquad (8)$$

$$\frac{dx_5}{dt} = -\frac{K_V}{T_V R_G} x_1 - \frac{1}{T_V} x_5 + \frac{K_V}{T_V} u_2. \qquad (9)$$

3.3 Small signal model equations of steam power plant with reheater in state space

By choosing four state variables, x_1 = frequency changes (Δf) , x_2 = turbine output mechanical power changes (ΔP_m) , x_3 = turbine output mechanical power changes without reheater and x_4 = steam valve changes, the first order differential equations representing the dynamic model of steam power plant with reheater are expressed as follows.

$$\frac{dx_1}{dt} = -\frac{K_D}{J_M} x_1 + \frac{1}{J_M} x_2 \pm \frac{1}{J_M} \sum \Delta P_{\text{tie}} -\frac{1}{J_M} u_1,$$
(10)

$$-\frac{1}{J_M}u_1, \qquad (10)$$

$$\frac{dx_2}{dt} = -\frac{1}{T_H}x_2 + \left(\frac{1}{T_H} - \frac{F_H}{T_T}\right)x_3 + \frac{F_H}{T_T}x_4, \qquad (11)$$

$$\frac{dx_3}{dt} = -\frac{1}{T_T}x_3 + \frac{1}{T_T}x_4\,, (12)$$

$$\frac{dx_4}{dt} = -\frac{K_G}{T_G R_S} x_1 - \frac{1}{T_G} x_4 + \frac{K_G}{T_G} u_2.$$
 (13)

Figure 4 shows the connection between three different areas. The output signal in each area is considered to be the frequency deviation of that area [51]. Therefore, depending on the power change of the connecting line between the areas, the number of state variables required to represent the connected power system – whether for a two-area or three-area system – will range from a minimum of 8 to a maximum of 16 [52].

4 Simulation Results and Discussion

Controlling the stability of frequency and terminal voltage at nominal values is crucial for the proper operation of an interconnected power system. In this section, the dynamic behavior of the load frequency control system in the interconnected power system, with different combinations of power plants, is simulated. The system modes are determined for each scenario, and the accuracy of the time-domain simulation results is validated based on these modes.

4.1 Single-area power system (areas independent function)

In this section, each power plant is treated as an independent area, separate from the others. The transient response of a single generation unit to a step change in load is shown in Figures 5 and 6. The modes of the multi-area power system, when each area operates independently, are presented in Table 5. As shown, the

response of each area to slight changes in load remains stable. The maximum frequency droop and its occurrence time for each power plant, in response to step changes in demand load, are presented in Table 6. As observed, the gas power plant exhibits the lowest frequency droop, while the hydro power plant shows the highest frequency droop. Furthermore, the gas power plant demonstrates a faster response compared to the other two power plants. The frequency droop after reaching the steady state is 0.1667 Hz for each power plant. Furthermore, the turbine output mechanical power for each power plant reaches 0.8333 pu in the steady state.

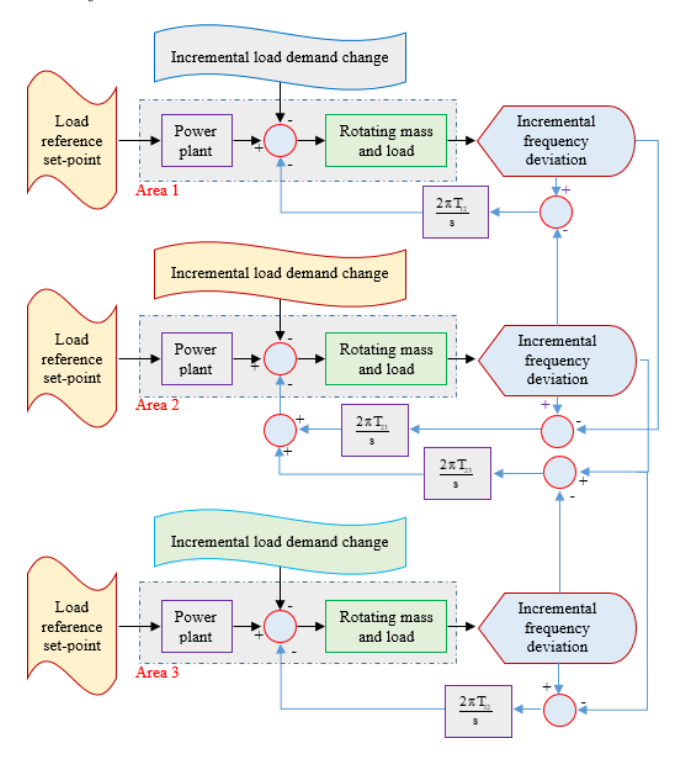


Fig. 4. Block diagram of a three-area interconnected power system.

Table 5. Power system modes of each area in separate operation.

Power plant	Eigenvalues in each area
Steam	$-5.2386, -2.558, -0.1909 \pm j0.2363$
Hydro	$-6.2203, -0.2066, -0.4225 \pm j0.8004$
Gas	-3.1534, -5.9059, -20.2748,
Gas	$-0.5961 \pm j0.6417$

Table 6. The amount of maximum frequency droop for step changes in demand load.

Power plant	Maximum frequency drop	Occurrence time
Steam	-0.2596	5.8330
Hydro	-0.3363	2.8800
Gas	-0.1863	3.2243

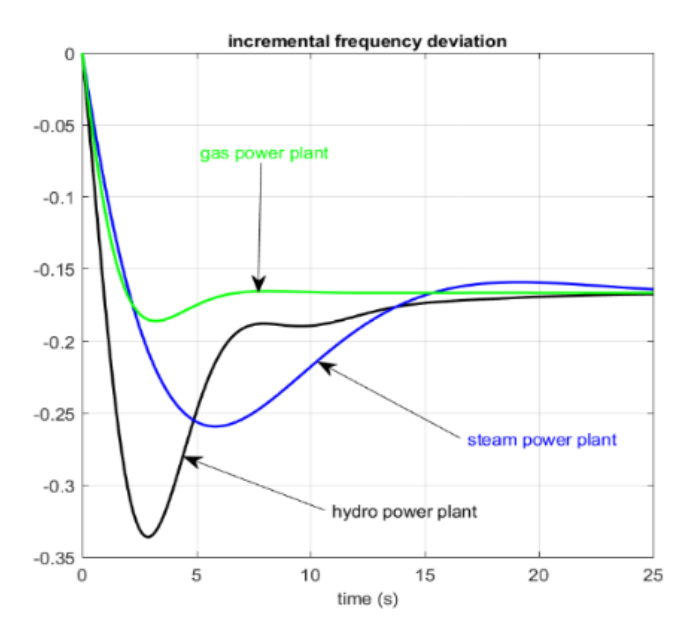


Fig. 5. Area frequency changes after step load disorder (areas independent function).

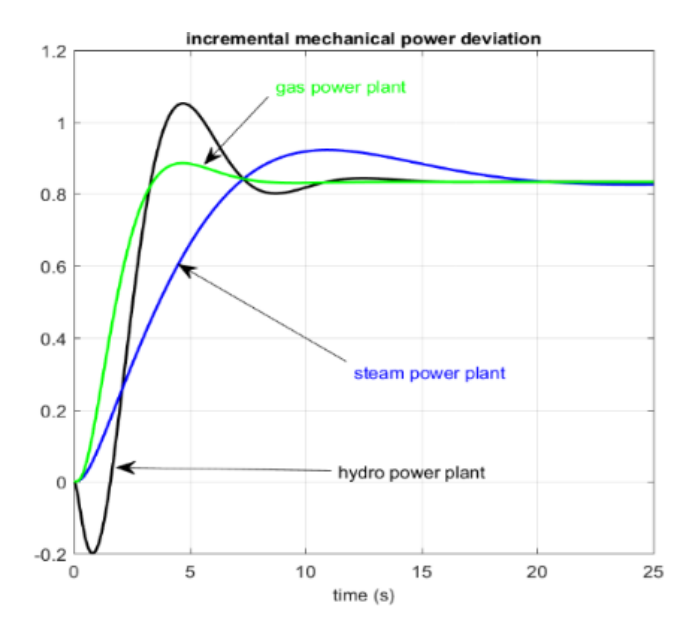


Fig. 6. Incremental changes in the output mechanical power of turbine after step load disorder (areas independent function).

4.2 Two-area power system (steam and hydro)

In this section, the power system consists of two areas: One with a steam power plant and the other with a hydro power plant. The dynamic behavior of the hydrothermal system in response to changes in demand load is presented. Figures 7 and 8 show the frequency changes in the areas following a step change in the demand load in the first area (steam power plant) and the second area (hydro power plant), respectively. Figure 9 illustrates the transmission power changes between the two areas in both cases. In the steady state, the frequency deviation in each area is -0.0832 Hz.

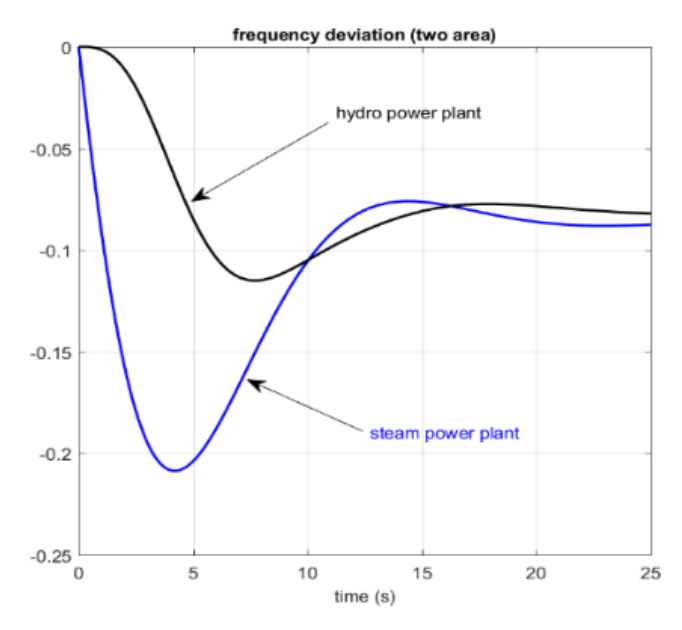


Fig. 7. Area frequency changes after step load disorder in area 1 (steam power plant) in scenario 1.

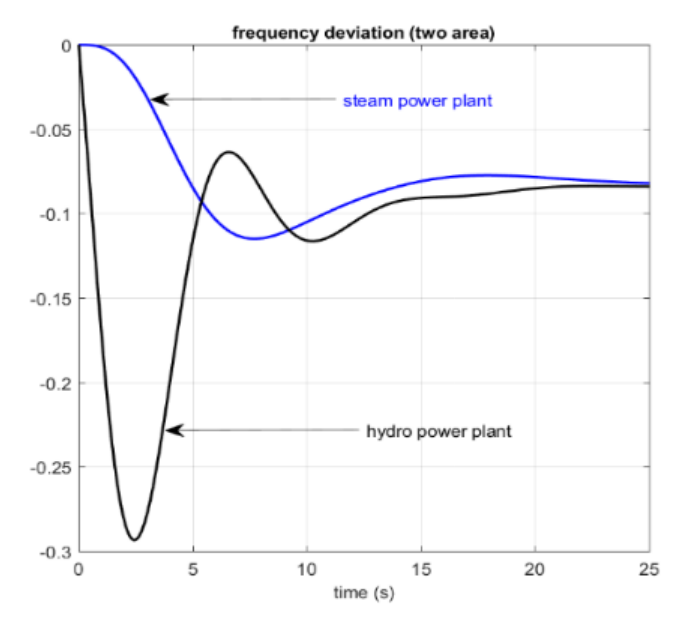


Fig. 8. Area frequency changes after step load disorder in area 2 (hydro power plant) in scenario 1.

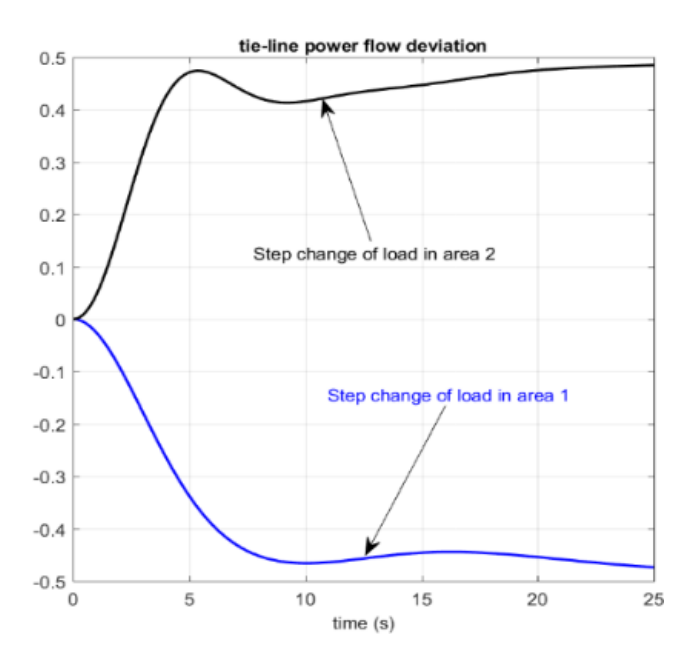


Fig. 9. Tie-line power flow changes after step load disorder in area 1 and area 2 in scenario 1.

4.3 Two-area power system (steam and gas)

The two most common power plants for electricity generation are steam and gas power plants. In this section, an interconnected power system consisting of two areas – one with a gas power plant and the other with a steam power plant – is considered. The frequency changes in each area, resulting from step changes in load demand in each area, are shown in Figures 10 and 11.

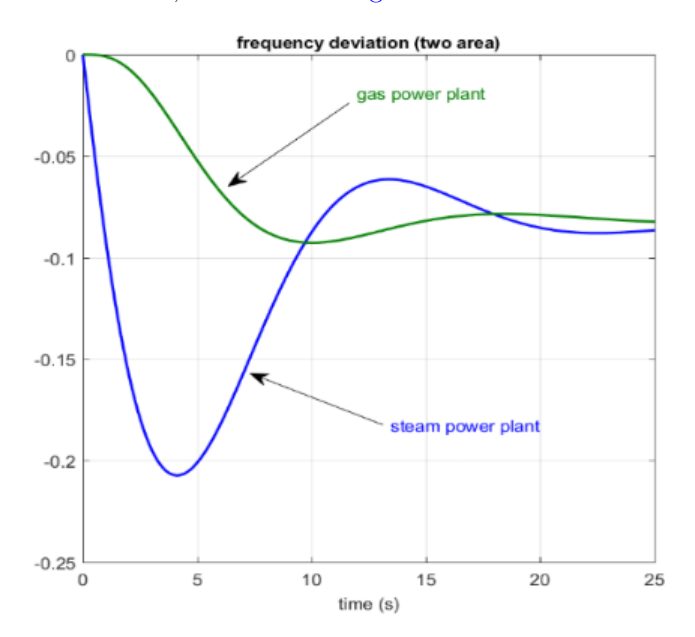


Fig. 10. Area frequency changes after step load disorder in area 1 (steam power plant) in scenario 2.

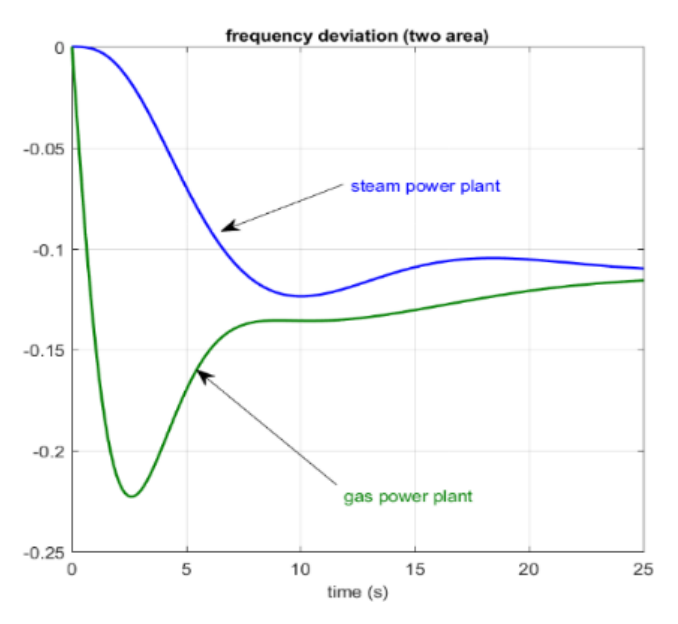


Fig. 11. Area frequency deviation after step load disorder in area 2 (gas power plant) in scenario 2.

Figure 12 illustrates the power changes in the tieline power flow between the two areas. When the load is changed in area 1, the frequency decreases to $0.833\,\mathrm{Hz}$ in steady state. In this case, the output mechanical power of the gas turbine and the steam turbine in steady state is $0.4167\,\mathrm{pu}$, and the inter-area power is $-0.5\,\mathrm{pu}$. When a step change in demand load occurs in Area 2, the frequency is reduced to $-0.1111\,\mathrm{Hz}$ in the steady state. In this case, the mechanical power of both turbines is $0.5556\,\mathrm{p.u.}$, and the power transfer between the two areas in steady state is $0.6667\,\mathrm{pu}$.

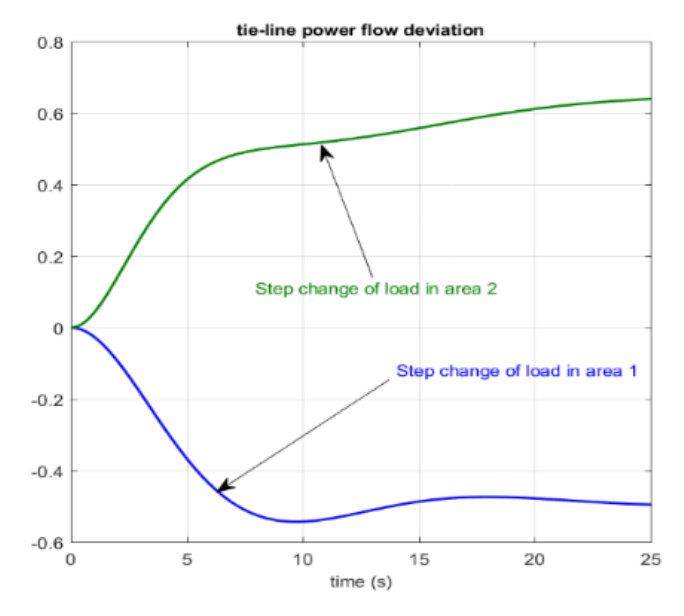


Fig. 12. Tie-line power flow deviation after step load disorder in area 1 and area 2 in scenario 2.

As observed from the simulation results, when load changes occur in Area 2 (i.e., the gas or hydro power plant), the frequency droop in Area 1 (the steam power plant) is greater. The gas power plant is well-suited for peak load demands, while the steam power plant is not as effective in handling peak loads.

4.4 Three-area interconnected power system

In this section, the connected power system consists of three areas as shown in Figure 13, with steam, hydro, and gas power plants forming the system. First, step changes in load are considered for Area 1, which is the hydro power plant.

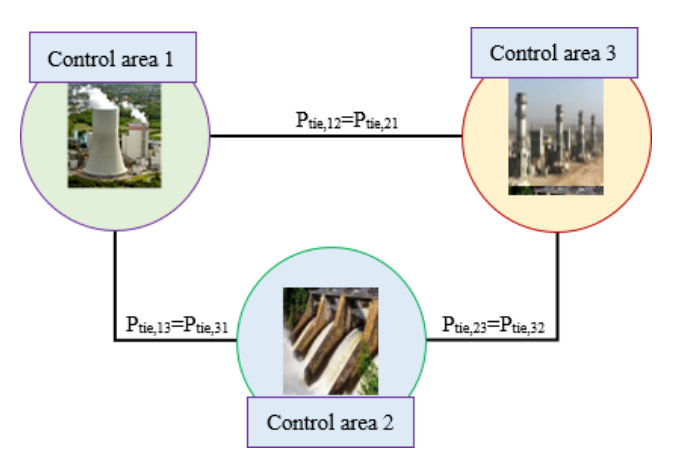


Fig. 13. Inter-area communication in a three-area interconnected power system.

The frequency changes for the three power plants are shown in Figure 14. As observed, the frequency droop in steady state is $-0.0556\,\mathrm{Hz}$. Figure 15 illustrates the power transfer between the regions. In the steady state, the power transfer between Areas 1 and 2 is $0.6663\,\mathrm{pu}$, and between Areas 2 and 3, it is $0.3331\,\mathrm{pu}$. Next, load changes in Area 2, which corresponds to the steam power plant, are considered. Figures 16 and 17 show the frequency changes across the three areas and the power changes between the areas, respectively.

To analyze and investigate the performance of the interconnected power system, the modes of the system matrix (eigenvalues of the system matrix) are listed in Table 7. As seen, the eigenvalues are located on the left side of the imaginary axis, which indicates that the power system is stable for slight changes in the demand load.

5 Conclusions

The consumption of active and reactive power is influenced by load changes or disturbances, which can significantly affect the normal operation of an interconnected power system. To maintain the frequency at its nominal value, a load frequency control (LFC) system is installed at the generating station. This system ensures that with changes in active power demand, the system frequency and the power transmitted through the connection lines remain within specified limits. Due to their rapid response, gas turbine units offer flexible tuning capabilities, making them valuable for stabilizing power systems.

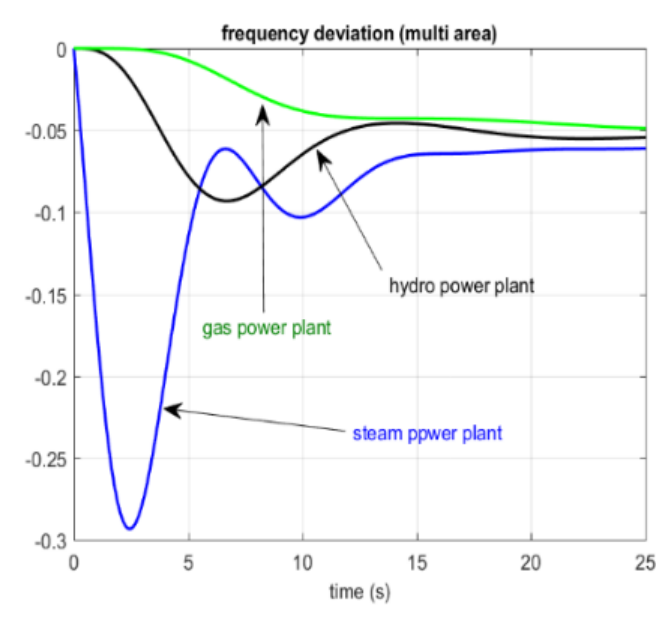


Fig. 14. Area frequency changes after step load disorder in area 1 (hydro power plant) in scenario 3.

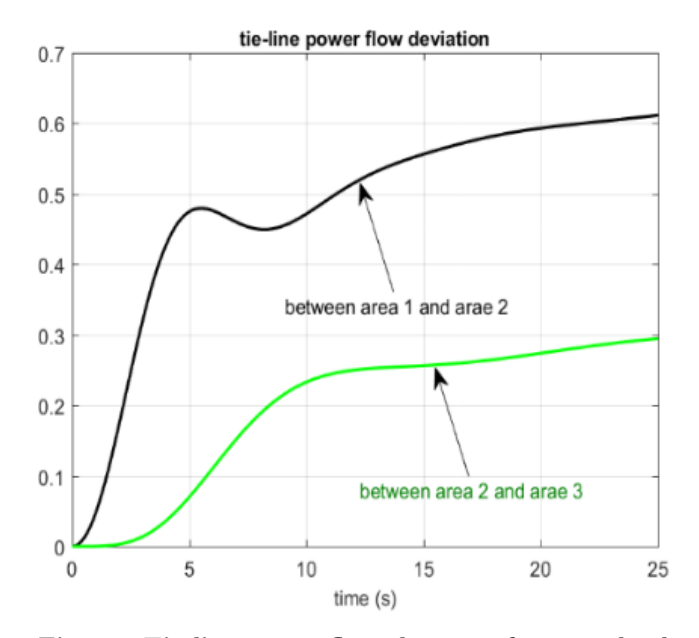
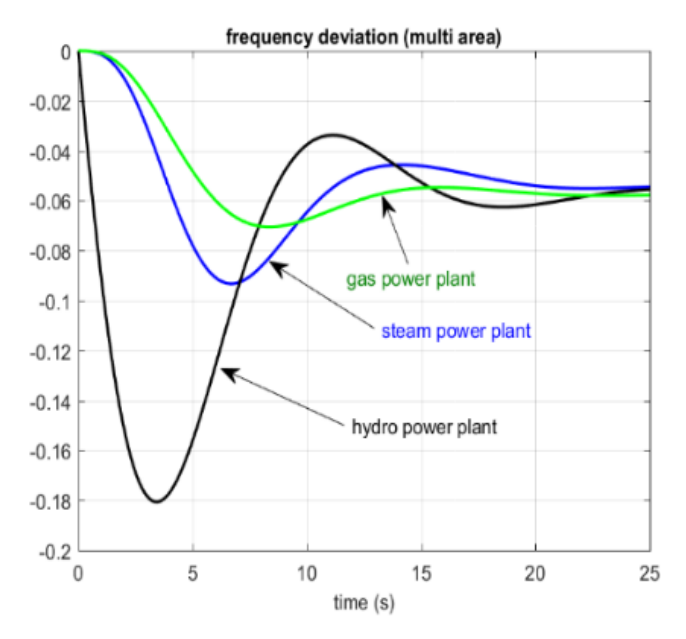


Fig. 15. Tie-line power flow changes after step load disorder in area 1 in scenario 3.



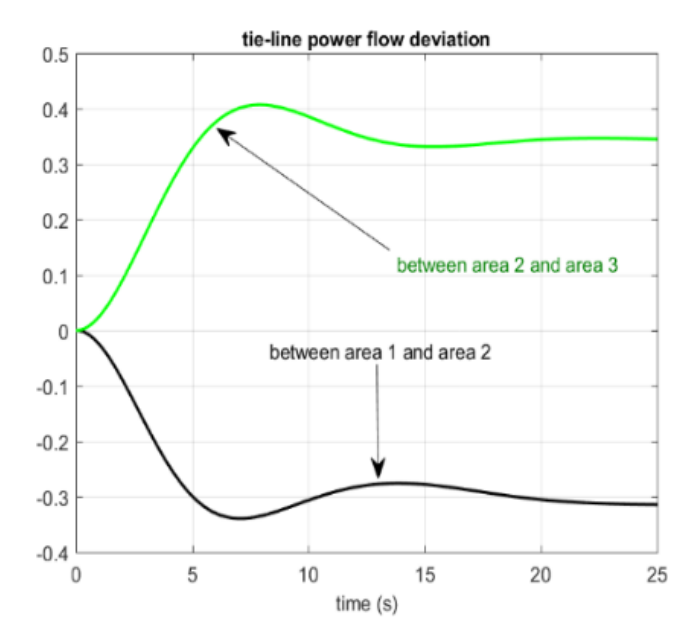


Fig. 16. Area frequency changes after step load disorder in area 2 (steam power plant) in scenario 3.

Fig. 17. Tie-line power flow changes after step load disorder in area 2 in scenario 3.

Table 7. Eigenvalues of the system matrix in the interconnected power system for different scenarios.

Combination of areas	Eigenvalues in interconnected power system
Steam + Hydro	$-0.0838, -0.2882, -2.9581, -5.2382, -6.2181, -0.2085 \pm j0.3250, -0.3223 \pm j0.8264$
45Steam + Gas	$-0.1186, -2.9580, -3.1582, -5.2382, -5.9048, -20.3748, -0.5435 \pm j0.6562,$
	$-0.1815 \pm j0.3407$
Steam + Hydro + Gas	-0.0678, -0.1205, -0.3020, -2.9602, -3.1582, -5.2378, -5.9048, -6.2181, -20.3748,
	$-0.5437 \pm j0.6557, -0.2000 \pm j0.4127, -0.3214 \pm j0.8257$

References

- [1] Yahyanezhad Gele M, Yaghmaei S, Mardanpour MM. A comparative study of three types of anode electrodes in a microfluidic microbial fuel cell. Hydrogen, Fuel Cell & Energy Storage. 2021;8(1):13–21.
- [2] Ghiasi MI, Aliakbar Golkar M, Hajizadeh A. Hierarchical Control Strategy of Heat and Power for Zero Energy Buildings including Hybrid Fuel Cell/Photovoltaic Power Sources and Plug-in Electric Vehicle. Hydrogen, Fuel Cell & Energy Storage. 2016;3(1):33–44.
- [3] Casati P, Moner-Girona M, Khaleel SI, Szabo S, Nhamo G. Clean energy access as an enabler for social development: A multidimensional analysis

- for Sub-Saharan Africa. Energy for Sustainable Development. 2023;72:114–126.
- [4] Rasaki S, Liu C, Lao C, Zhang H, Chen Z. The innovative contribution of additive manufacturing towards revolutionizing fuel cell fabrication for clean energy generation: A comprehensive review. Renewable and sustainable energy reviews. 2021;148:111369.
- [5] Aghadavoodi E, Shahgholian G. A new practical feed-forward cascade analyze for close loop identification of combustion control loop system through RANFIS and NARX. Applied Thermal Engineering. 2018;133:381–395.
- [6] Fathollahi A, Gheisarnejad M, Andresen B, Farsizadeh H, Khooban MH. Robust artificial intelli-

- gence controller for stabilization of full-bridge converters feeding constant power loads. IEEE Transactions on Circuits and Systems II: Express Briefs. 2023;70(9):3504–3508.
- [7] Ghazanfar S. Modeling and Simulation of a Twomass Resonant System with Speed Controller. International Journal of Information and Electronics Engineering. 2013;3(5):449–452.
- [8] Khalil AE, Boghdady TA, Alham M, Ibrahim DK. A novel cascade-loop controller for load frequency control of isolated microgrid via dandelion optimizer. Ain Shams Engineering Journal. 2024;15(3):102526.
- [9] Jin Y, Behrens P, Tukker A, Scherer L. Water use of electricity technologies: A global metaanalysis. Renewable and Sustainable Energy Reviews. 2019;115:109391.
- [10] Kabeyi MJB, Olanrewaju OA. The levelized cost of energy and modifications for use in electricity generation planning. Energy Reports. 2023;9:495– 534.
- [11] Izanlo A, Gholamian SA, Kazemi MV. Comparative study between two sensorless methods for direct power control of doubly fed induction generator. Rev Roum Sci Techn-Electrotechn Et Energ. 2017;62(4):358–364.
- [12] Fathollahi A, Andresen B. Deep deterministic policy gradient for adaptive power system stabilization and voltage regulation. e-Prime-Advances in Electrical Engineering, Electronics and Energy. 2024;9:100675.
- [13] Li B, Hu S, Zhong Q, Shi K, Zhong S. Dynamic memory event-triggered proportional-integral-based H_{∞} load frequency control for multi-area wind power systems. Applied Mathematics and Computation. 2023;453:128070.

- [14] Fooladgar M, Fani B, Shahgholian G, et al. Evaluation of the trajectory sensitivity analysis of the DFIG control parameters in response to changes in wind speed and the line impedance connection to the grid DFIG. Journal of Intelligent Procedures in Electrical Technology. 2015;5(20):37–54.
- [15] Zhao X, Ma Z, Zou S, Shi X. Distributed optimal load frequency control for multi-area power systems with controllable loads. Journal of the Franklin Institute. 2024;p. 107007.
- [16] Masikana S, Sharma G, Sharma S. Renewable Energy Sources Integrated Load Frequency Control of Power System: A Review. e-Prime-Advances in Electrical Engineering, Electronics and Energy. 2024;p. 100605.
- [17] Jia Y, Dong ZY, Sun C, Meng K. Cooperation-based distributed economic MPC for economic load dispatch and load frequency control of inter-connected power systems. IEEE Transactions on Power Systems. 2019;34(5):3964–3966.
- [18] Latif A, Hussain SS, Das DC, Ustun TS. State-of-the-art of controllers and soft computing techniques for regulated load frequency management of single/multi-area traditional and renewable energy based power systems. Applied Energy. 2020;266:114858.
- [19] Ali T, Malik SA, Hameed IA, Daraz A, Mujlid H, Azar AT. Load frequency control and automatic voltage regulation in a multi-area interconnected power system using nature-inspired computation-based control methodology. Sustainability. 2022;14(19):12162.
- [20] Xiong J, Ding Y, Ye H, Pei W, Kong L. The additional control strategies to improve primary frequency response for hybrid power plant with gas turbines and steam turbines. Energy Reports. 2022;8:557–564.

- [21] Qiao S, Liu X, Wang D, Ge SS. Security Concern and Fuzzy Output Sliding Mode Load Frequency Control of Power Systems. Information Sciences. 2024;p. 120793.
- [22] Zhong Q, Hu S, Yan L, Zhou H, Yang J, Shi K, et al. Adaptive event-triggered PID load frequency control for multi-area interconnected wind power systems under aperiodic DoS attacks. Expert Systems with Applications. 2024;241:122420.
- [23] Rajan R, Fernandez FM. Small-signal stability analysis and frequency regulation strategy for photovoltaic sources in interconnected power system. Electrical Engineering. 2021;103(6):3005–3021.
- [24] Aluko AO, Carpanen RP, Dorrell DG, Ojo EE. Robust state estimation method for adaptive load frequency control of interconnected power system in a restructured environment. IEEE Systems Journal. 2020;15(4):5046–5056.
- [25] Ray PK, Bartwal A, Puhan PS. Load frequency control in interconnected microgrids using Hybrid PSO-GWO based PI-PD controller. International Journal of System Assurance Engineering and Management. 2024;15(8):4124-4142.
- [26] Guo J. A Novel Proportional-Derivative Sliding Mode for Load Frequency Control. IEEE Access. 2024;.
- [27] Zhang J, Peng F, Wang L, Yang Y, Li Y. A load frequency control strategy based on double deep Q-network and upper confidence bound algorithm of multi-area interconnected power systems. Computers and Electrical Engineering. 2024;120:109778.
- [28] Ali T, Asad M, Touti E, Graba BB, Aoudia M, Abbas G, et al. Terminal Voltage and Load Frequency Control in a Real Four-Area Multi-Source Interconnected Power System With Nonlinearities via OOBO Algorithm. IEEE Access. 2024;.

- [29] Mufti Mud, Lone SA, Iqbal SJ, Mushtaq I. Improved load frequency control with superconducting magnetic energy storage in interconnected power systems. IEEJ Transactions on Electrical and Electronic Engineering. 2007;2(3):387–397. Available from: https://onlinelibrary.wiley.com/doi/abs/10.1002/tee.20160.
- [30] Zeng GQ, Xie XQ, Chen MR. An adaptive model predictive load frequency control method for multi-area interconnected power systems with photovoltaic generations. Energies. 2017;10(11):1840.
- [31] Yang M, Wang C, Hu Y, Liu Z, Yan C, He S. Load frequency control of photovoltaic generation-integrated multi-area interconnected power systems based on double equivalent-input-disturbance controllers. Energies. 2020;13(22):6103.
- [32] Khalil AE, Boghdady TA, Alham M, Ibrahim DK. A novel multi-objective tuning formula for load frequency controllers in an isolated low-inertia microgrid incorporating PV/wind/FC/BESS. Journal of Energy Storage. 2024;82:110606.
- [33] Hakimuddin N, Nasiruddin I, Bhatti TS, Arya Y. Optimal automatic generation control with hydro, thermal, gas, and wind power plants in 2-area interconnected power system. Electric Power Components and Systems. 2020;48(6-7):558–571.
- [34] Zheng Y, Tao J, Sun Q, Sun H, Chen Z, Sun M. Deep reinforcement learning based active disturbance rejection load frequency control of multi-area interconnected power systems with renewable energy. Journal of the Franklin Institute. 2023;360(17):13908–13931.
- [35] Ahmed EM, Mohamed EA, Selim A, Aly M, Alsadi A, Alhosaini W, et al. Improving load frequency control performance in interconnected

- power systems with a new optimal high degree of freedom cascaded FOTPID-TIDF controller. Ain Shams Engineering Journal. 2023;14(10):102207.
- [36] Fani B, Mesrinejad F, Yaghoubi S, Alhelou H. Improved Dynamic Performance in Interconnected Power System Using Secondary Frequency Control. International Journal of Smart Electrical Engineering. 2023;12(02):127–133.
- [37] Mesrinejad F, Yaghoubi S, Fani B. Secondary frequency control for improved dynamic performance in interconnected power system. Journal of Simulation and Analysis of Novel Technologies in Mechanical Engineering. 2022;14(4):5–12.
- [38] Patre B, Londhe P, Nagarale R. Fuzzy sliding mode control for spatial control of large nuclear reactor. IEEE Transactions on Nuclear Science. 2015;62(5):2255–2265.
- [39] Kunya AB. Hierarchical bi-level load frequency control for multi-area interconnected power systems. International Journal of Electrical Power & Energy Systems. 2024;155:109600.
- [40] Bevrani H, Golpîra H, Messina AR, Hatziargyriou N, Milano F, Ise T. Power system frequency control: An updated review of current solutions and new challenges. Electric Power Systems Research. 2021;194:107114.
- [41] Kerdphol T, Rahman FS, Mitani Y. Virtual inertia control application to enhance frequency stability of interconnected power systems with high renewable energy penetration. Energies. 2018;11(4):981.
- [42] Li J, Dai J, Cui H. Bionic cooperative load frequency control in interconnected grids: A multi-agent deep Meta reinforcement learning approach. Applied Energy. 2025;379:124906.
- [43] Li J, Zhou T. Bio-inspired distributed load frequency control in Islanded Microgrids: A multi-

- agent deep reinforcement learning approach. Applied Soft Computing. 2024;166:112146.
- [44] Ji X, Luo H, Cao K, Liu D, Xiong P. Multiobjective design of fractional frequency-load control for hydro-thermal system considering nonlinear models and uncertainty. Ain Shams Engineering Journal. 2024;15(12):103137.
- [45] Mustafa GI, Masum M, Siam M. A new modelfree control for load frequency control of interconnected power systems based on nonlinear disturbance observer. Energy Reports. 2024;12:4998– 5008.
- [46] Haq IU, Rahman A, Hussain SS. Impact of network degradation on load frequency control of large interconnected power system. Computers and Electrical Engineering. 2024;118:109394.
- [47] Shukla RR, Garg MM, Panda AK, Das D. Enhancing load frequency control with plug-in electric vehicle integration in non-reheat thermal power systems. Electrical Engineering. 2024;106(3):3305–3320.
- [48] Kalyan CNS, Suresh CV. Higher order degree of freedom controller for load frequency control of multi area interconnected power system with time delays. Global Transitions Proceedings. 2022;3(1):332–337.
- [49] Zhu F, Zhou X, Zhang Y, Xu D, Fu J. A load frequency control strategy based on disturbance reconstruction for multi-area interconnected power system with hybrid energy storage system. Energy Reports. 2021;7:8849–8857.
- [50] Shahgholian G. Power system stabilizer application for load frequency control in hydroelectric power plant. Engineering Mathematics. 2017;2(1):21–30.
- [51] Chen G, Li Z, Zhang Z, Li S. An improved ACO algorithm optimized fuzzy PID controller

for load frequency control in multi area interconnected power systems. Ieee Access. 2019;8:6429–6447.

[52] Shahgholian G, Fathollahi A. Analyzing small-

signal stability in a multi-source single-area power system with a load-frequency controller coordinated with a photovoltaic system. AppliedMath. 2024;4(2):452-467.